REPORT DOCUMENTATION PAGE

Form Approved
OMB No. 0704-0188

1. AGENCY USE ONLY *(Leave blank)*	2. REPORT DATE	3. REPORT TYPE AND DATES COVERED
	9 Jan 97	

4. TITLE AND SUBTITLE
Alterations In Nerve Terminal Arborization Do Not Correlate With Increased Synaptic Efficacy In the Lobster Neuromuscular Junction.

5. FUNDING NUMBERS

6. AUTHOR(S)
Timothy P. schultz

7. PERFORMING ORGANIZATION NAME(S) AND ADDRESS(ES)
Colorado State University

8. PERFORMING ORGANIZATION REPORT NUMBER
96-108

9. SPONSORING/MONITORING AGENCY NAME(S) AND ADDRESS(ES)
DEPARTMENT OF THE AIR FORCE
AFIT/CI
2950 P STREET
WPAFB OH 45433-7765

10. SPONSORING/MONITORING AGENCY REPORT NUMBER

11. SUPPLEMENTARY NOTES

12a. DISTRIBUTION AVAILABILITY STATEMENT
Unlimited

12b. DISTRIBUTION CODE

13. ABSTRACT *(Maximum 200 words)*

14. SUBJECT TERMS	15. NUMBER OF PAGES
	44
	16. PRICE CODE

17. SECURITY CLASSIFICATION OF REPORT	18. SECURITY CLASSIFICATION OF THIS PAGE	19. SECURITY CLASSIFICATION OF ABSTRACT	20. LIMITATION OF ABSTRACT

DISCLAIMER NOTICE

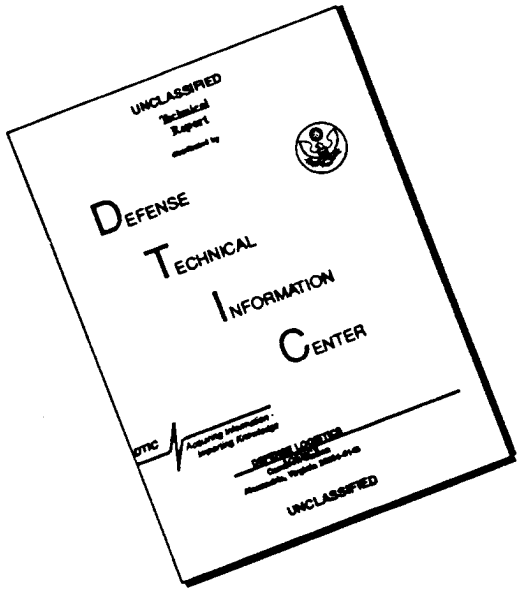

THIS DOCUMENT IS BEST QUALITY AVAILABLE. THE COPY FURNISHED TO DTIC CONTAINED A SIGNIFICANT NUMBER OF PAGES WHICH DO NOT REPRODUCE LEGIBLY.

ABSTRACT OF THESIS

ALTERATIONS IN NERVE TERMINAL ARBORIZATION DO NOT CORRELATE WITH INCREASED SYNAPTIC EFFICACY IN THE LOBSTER NEUROMUSCULAR JUNCTION

Neurotransmitter release is essential for chemical synaptic transmission, and the efficacy of synaptic transmission depends on how much transmitter is released from discrete sites in the axon terminal called active zones. The number and structural organization of active zones are important for governing synaptic efficacy, and may play a central role in synaptic plasticity. One method to enhance synaptic strength could be to expand the nerve terminal arborization to accommodate an increase in the number of active zones. The possibility that experimentally induced increases in synaptic efficacy correlate with increases in the amount of nerve terminal arborization is tested in this Master of Science Thesis.

The lobster distal accessory flexor muscle (DAFM) is an excellent model for studying the relationship between synaptic efficacy and the structural organization of the presynaptic axon terminal A single excitatory and inhibitory motor neuron innervate the DAFM, and the amount of transmitter they release is regionally differentiated. Regional differences in both the number and structure of active zones contribute to the regional differences in the amount of transmitter released. This investigation uses a fluorescent dye

(FM1-43) to label motor axon terminals in the DAFM, and the terminal arborizations of these neurons are reconstructed in three dimensions using a confocal laser scanning fluorescent microscope. The extent of neuronal innervation is quantified in these images, and measurements of both synaptic efficacy and the size of the fluorescently labeled terminal arborizations from experimental preparations are compared to controls. The results confirm that a significant increase in synaptic efficacy is not accompanied by a significant alteration in the area of muscle fiber membrane occupied by nerve terminal arborization. These results suggest that increases in synaptic efficacy may result from alterations in synaptic structure such as increases in active zone number within a fixed presynaptic area or alterations in active zone structure.

Timothy P. Schultz
Anatomy and Neurobiology Department
Colorado State University
Fort Collins, CO 80523
Fall 1996

THESIS

ALTERATIONS IN NERVE TERMINAL ARBORIZATION DO NOT CORRELATE WITH INCREASED SYNAPTIC EFFICACY IN THE LOBSTER NEUROMUSCULAR JUNCTION

Submitted by
Timothy P. Schultz
Anatomy and Neurobiology Department

In partial fulfillment of the requirements
for the Degree of Master of Science
Colorado State University
Fort Collins, Colorado
Fall 1996

COLORADO STATE UNIVERSITY

22 November 1996

WE HEREBY RECOMMEND THAT THE THESIS PREPARED UNDER OUR SUPERVISION BY TIMOTHY P. SCHULTZ ENTITLED "ALTERATIONS IN NERVE TERMINAL ARBORIZATION DO NOT CORRELATE WITH INCREASED SYNAPTIC EFFICACY IN THE LOBSTER NEUROMUSCULAR JUNCTION" BE ACCEPTED AS FULFILLING IN PART REQUIREMENTS FOR THE DEGREE OF MASTER OF SCIENCE.

Committee on Graduate Work

Donald L. Myklebust

Adviser

Department Head

ABSTRACT OF THESIS

ALTERATIONS IN NERVE TERMINAL ARBORIZATION DO NOT CORRELATE WITH INCREASED SYNAPTIC EFFICACY IN THE LOBSTER NEUROMUSCULAR JUNCTION

Neurotransmitter release is essential for chemical synaptic transmission, and the efficacy of synaptic transmission depends on how much transmitter is released from discrete sites in the axon terminal called active zones. The number and structural organization of active zones are important for governing synaptic efficacy, and may play a central role in synaptic plasticity. One method to enhance synaptic strength could be to expand the nerve terminal arborization to accommodate an increase in the number of active zones. The possibility that experimentally induced increases in synaptic efficacy correlate with increases in the amount of nerve terminal arborization is tested in this Master of Science Thesis.

The lobster distal accessory flexor muscle (DAFM) is an excellent model for studying the relationship between synaptic efficacy and the structural organization of the presynaptic axon terminal A single excitatory and inhibitory motor neuron innervate the DAFM, and the amount of transmitter they release is regionally differentiated. Regional differences in both the number and structure of active zones contribute to the regional differences in the amount of transmitter released. This investigation uses a fluorescent dye

differences in the amount of transmitter released. This investigation uses a fluorescent dye (FM1-43) to label motor axon terminals in the DAFM, and the terminal arborizations of these neurons are reconstructed in three dimensions using a confocal laser scanning fluorescent microscope. The extent of neuronal innervation is quantified in these images, and measurements of both synaptic efficacy and the size of the fluorescently labeled terminal arborizations from experimental preparations are compared to controls. The results confirm that a significant increase in synaptic efficacy is not accompanied by a significant alteration in the area of muscle fiber membrane occupied by nerve terminal arborization. These results suggest that increases in synaptic efficacy may result from alterations in synaptic structure such as increases in active zone number within a fixed presynaptic area or alterations in active zone structure.

Timothy P. Schultz
Anatomy and Neurobiology Department
Colorado State University
Fort Collins, CO 80523
Fall 1996

ACKNOWLEDGMENTS

I would like to thank my advisor, Dr. John Walrond, for his guidance, advice, and patience throughout this project and for making my graduate education even more enjoyable. I would also like to thank my other committee members, Dr. Don Mykles and Dr. John Rash, for their input, patience, and expertise. Further thanks goes to Scott Druecker for his expert training in dissection methods and for his electrophysiology work used in this thesis. Other members of the Walrond lab, Pete Dobelis, Elizabeth Alexander, and Irene Mayer, also provided valuable support and assistance. I also thank Dr. John Chandler and Tom Yasumura for their technical expertise with the confocal microscope and imaging systems. Sincere thanks also go to Anna Fails as well as Eileen Diepenbrock and her outstanding office staff for their help and good humor.

Many thanks go to family and friends. I would especially like to thank my lovely and wonderfully patient wife, Stacie. Without her love and support, this project and my sanity would both be lost.

Finally, I give my utmost thanks to Jesus Christ for His love and grace. With Him, all things are possible.

> For since the creation of the world, God's invisible qualities--his eternal power and divine nature--have been clearly seen, being understood from what has been made, so that men are without excuse. Romans 1:20.
>
> And we know that in all things God works for the good of those who love Him, who have been called according to His purpose. Romans 8:28

TABLE OF CONTENTS

INTRODUCTION

The aim of this study is to provide insight into a fundamental problem in neurobiology: how the nervous system effects long term changes in synaptic connectivity and output among a fixed number of neurons. Much of our understanding of synaptic function and plasticity comes from the cellular analysis of the physiological and morphological properties of chemical synaptic transmission. The invertebrate neuromuscular junction, which provides an excellent paradigm for studying the structure and function of chemical synapses at the cellular level, is recognized as a model for synapses in the vertebrate central nervous system (Katz, 1966). This thesis uses the crustacean neuromuscular junction to investigate the relationship between increases in synaptic efficacy and alterations in the size of motor axon terminal arborizations.

Background

Intercellular communication among neurons occurs primarily at chemical synapses and is fundamental to nervous system function. Chemical synaptic transmission employs a complex cascade of events to transduce signals between pre- and postsynaptic cells, and alterations in synaptic connectivity appear to be important for effecting changes in the output of nervous systems (Bailey and Kandel, 1993). The neuromuscular junction

is a highly specialized synapse and provides an important model for characterizing physiological and morphological properties essential in chemical synaptic transmission (Rash et al., 1988). Mechanisms for synaptic transmission appear to be similar at peripheral and central nervous system synapses in vertebrates and invertebrates (Katz, 1966), and morphological and physiological studies on invertebrate neuromuscular synapses have provided important insights into the cellular basis of synaptic transmission and synaptic plasticity (for review see Bailey and Kandel, 1993). Although alterations in synaptic structure and function are thought to play a role in learning and memory in higher vertebrates, the complexity of the mammalian brain makes these studies extremely difficult. At invertebrate neuromuscular junctions, a relatively small number of identifiable motor neurons synapse onto muscle fibers and are well-suited for electrophysiological and morphological analysis. These motor neurons vary the amount of transmitter they release over a broad range and exhibit long-term changes in synaptic transmission (Lnenicka et al., 1986; Walrond et al., 1993; Atwood et al., 1994). Therefore, invertebrate neuromuscular junctions provide excellent model systems for studying the morphological and physiological correlates of long-term changes in synaptic efficacy.

The release of neurotransmitter in packets containing several thousand molecules is a fundamental property of chemical synaptic transmission known as quantal transmitter release. At vertebrate neuromuscular junctions, the release of excitatory neurotransmitter from the motor neuron depolarizes the postsynaptic cell (Fatt and Katz, 1952; del Castillo and Katz, 1954; Katz, 1962). The minimum amplitude of these depolarizations (or postsynaptic potentials) is usually about 0.5 mV, and the amplitudes of the larger

postsynaptic potentials are incremented in 0.5 mV steps (Fatt and Katz, 1952; del Castillo and Katz, 1954). According to Katz and coworkers, this incremental relationship is a function of quantal transmitter release, and the size of the postsynaptic potential depends on the number of quanta that are released nearly simultaneously during a nerve terminal depolarization. Normally, postsynaptic potentials in vertebrate skeletal muscle result from the release of 100-300 quanta (del Castillo and Katz, 1954), and the number of quanta released is referred to as the "quantal content" (Katz, 1969). The influx of extracellular calcium into the presynaptic axon terminal is necessary for quantal transmitter release (Katz and Miledi, 1967), and the quantal content varies with the fourth power of the calcium concentration (Dodge and Rahamimoff, 1967; Augustine et al., 1985; Adler et al., 1991).

Presynaptic axon terminals contain numerous 30-50 nm diameter synaptic vesicles, and several lines of evidence indicate that each synaptic vesicle contains one quantum (5,000-10,000 molecules) of neurotransmitter (for a review, see Rash et al., 1988). Quantal transmitter release occurs in response to an influx of calcium when synaptic vesicles fuse with the plasma membrane at distinct sites called active zones (Couteaux and Pecot-Dechavassine, 1970; Heuser et al., 1974, 1979). Active zones are recognized in thin sections as presynaptic densities adjacent to the plasma membrane, and are flanked by synaptic vesicles lying apposed to the plasma membrane (Couteaux and Pecot-Dechavassine, 1970; Hueser and Reese, 1973; Heuser et al., 1979). These vesicles are presumed to be the ones that fuse with the plasma membrane in response to a depolarization-induced calcium influx (Heuser et al., 1979).

In freeze-fracture views, active zones are visible as arrays of large intramembrane particles (active zone particles) in the protoplasmic leaflet of the presynaptic membrane (Dryer et al., 1973; Heuser et al., 1974; Gulley et al., 1978; Pearce et al., 1986; Roberts et al., 1990). Because there is only a brief delay (about 200 μsec) between calcium influx and the initiation of the postsynaptic response, the calcium channels that govern transmitter release must be located within 100 nm of the transmitter release sites (Llinas et al., 1981). The location of active zone particles within 100 nm of the transmitter release sites (Pumplin et al., 1981; Walrond and Reese, 1985) and the requirement for calcium to trigger transmitter release (Fatt and Katz, 1952; del Castillo and Katz, 1954; Katz and Miledi, 1967) indicate that active zone particles likely include the calcium channels that link the presynaptic action potential to transmitter release. Taken together, these morphological and physiological properties suggest that the locus of control for transmitter release is the active zone.

Structural Mechanisms Affecting Synaptic Plasticity

The structure of active zones plays a role in governing the amount of neurotransmitter released and thereby influences synaptic strength. Altering active zone structure by increasing the number of voltage-gated calcium channels clustered at the active zone appears to yield a greater than linear increase in the amount of transmitter released (Walrond and Reese, 1985; Walrond et al., 1993). At the frog neuromuscular junction, contralateral denervation increases synaptic efficacy three to eight fold without producing a corresponding morphological change visible in the light microscope (Herrera

and Grinnel, 1981). The ultrastructural correlate for this increase appears to be a change in active zone size, as identified from reconstructions of semiserial thin sections (Herrera et al., 1985). Propst and Ko (1987) also compared synaptic efficacy with active zone structure at the same synapse and concluded that the number of active zone particles positively correlates with quantal content in the frog neuromuscular junction. An increase in active zone size is also associated with both long-term potentiation in the hippocampal dentate gyrus (Desmond and Levy, 1988) and increased synaptic strength in *Aplysia* sensory to motor neuron synapses (Bailey and Chen, 1983; Wernig and Herrera, 1986). At crustacean neuromuscular junctions, differences in synaptic strength are associated with differences in active zone number and structure (Govind and Chiang, 1979; Govind and Meiss, 1979; Meiss and Govind, 1979, 1980; Atwood and Marin, 1983; Rheuben, 1985 Walrond et al., 1993). Therefore, morphological alterations that effect long-term changes in synaptic strength are likely to be localized at active zones as either changes in number or structure.

Several examples show how changing the number of active zones may be an important factor influencing synaptic strength. Most crustacean neuromuscular synapses are located in swellings along axonal branches called varicosities, and a varicosity contains several synapses (Florey and Cahill, 1983; Walrond et al., 1993). A synapse is conventionally defined in arthropods as a "continuous area of darkly stained pre- and postsynaptic membrane with uniform separation seen with the electron microscope" that may contain zero, one, or more active zones (Stewart et al., 1996). Transmitter release characteristics of crayfish nerve terminals correspond to the number of active zones per synapse (Cooper et al., 1995). In *Drosophila* mutants where the size of the motor axon

terminal arborization is reduced, synaptic strength is maintained at control levels by increasing the number of active zones per synapse and by increasing the number of synapses per unit area of terminal (Stewart et al., 1996). Increases in synaptic efficacy in other *Drosophila* mutants are associated with reductions in the number of varicosities and terminal axon branches; the morphological correlates of these changes are unknown (Zhong and Shanley, 1995). In humans with Lambert-Eaton myasthenic syndrome, reductions in quantal transmitter release correlate with reductions in active zone number and disruption of active zone organization (Fukunaga et al., 1982, 1983; Garcia et al., 1996). Therefore, alterations in both active zone number and active zone organization appear to influence synaptic efficacy.

Changing the number of active zones by altering the size of the axon terminal is another means of affecting synaptic input and changing synaptic efficacy. Sprouting of mature axons is a well known consequence of partial denervation in vertebrate muscle (Brown et al., 1981); adult motor neurons also generate numerous collateral or terminal sprouts in response to conditions such as growth, altered use, aging, and exposure to pathogens (Wernig and Herrera, 1986). Activity-related changes in neuronal morphology are also seen in the mammalian CNS; for example, changes in environmental stimuli evoke a 25-40% increase in the extent and branching of dendrites and a comparable change in the number of synapses per neuron in mammalian brain (for a review see Bailey and Kandel, 1993). Similar rearrangements are observed in some forms of synaptic plasticity in invertebrates. For example, long-term sensitization in *Aplysia* is accompanied by a doubling in the number of varicosities and an increase in axonal arborization (Bailey and Chen, 1988a,b, 1989). Also, an increase in the size and number

of synaptic varicosities in crustacean tonic motor axon terminals accompanies an increase in synaptic efficacy (Lnenicka et al., 1988). *Drosophila* mutants with reduced potassium conductance have larger motor axon terminal arborizations than wild-type flies (Budnik et al., 1990). Furthermore, in the adult lobster DAFM a ten-fold increase in weight is accompanied by a two-fold increase in quantal transmitter release, and the rise in transmitter output coincides with increases in the number of nerve terminals, synapses, and active zones (Pearce et al., 1985). Clearly, expanding the synaptic area is a commonly used mechanism to facilitate increases in synaptic efficacy.

There are many similarities between crustaceans and insects in regard to the physiology and morphology of synaptic transmission, and the strategies employed to effect increases in synaptic efficacy may be similar in these two classes of invertebrates. Studies of synaptic plasticity in *Drosophila* have used mutations that affect neuronal activity (Budnik et al., 1990), and provide insight into the relationship between synaptic plasticity and morphology in crustaceans. For example, the increased levels of transmitter release in hyperexcitable mutants is associated with an increase in both the number of axon branches and varicosities (Budnik et al., 1990). These results are consistent with axonal sprouting accounting for increased transmitter release. Axonal sprouting cannot provide a complete explanation for synaptic plasticity since mutants that lack expression of the cell adhesion molecule Fasciclin I display increased nerve terminal arborizations yet show reduced levels of transmitter release. Conversely, mutants that overexpress Fasciclin I have decreased terminal arborizations and increased transmitter release as compared to controls (Zhong and Shanley, 1995).

Studies involving another cell adhesion molecule, Fasciclin II, also suggest that the size of the motor axon terminal arborization and synaptic efficacy are independent since Fas II mutants have a reduced number of nerve terminal varicosities but show no change in transmitter release. Although the size of the nerve terminal arborization was decreased in Fas II mutants, the motor axon terminals contained larger synapses and a greater number of active zones per synapse (Stewart et al., 1996). The studies in *Drosophila* link changes in synaptic strength with changes in synaptic morphology, and suggest that synaptic plasticity is not tied to a particular structural parameter. Crustaceans may fall into a similar category and use any one or a combination of structural characteristics to effect changes in synaptic strength. The lobster distal accessory flexor muscle (DAFM) provides an excellent system to test these postulates because the morphological correlates for differences in synaptic efficacy are well characterized in this muscle.

The Lobster as a Model System

One or more of these morphological alterations could be responsible for experimentally induced changes in synaptic efficacy in the lobster (*Homarus americanus*). In the DAFM of the lobster walking leg (Fig. 1), one excitatory and one inhibitory motor neuron innervate the entire muscle (Govind and Pearce, 1982). The branch of the excitatory neuron innervating the most distal muscle fiber bundle releases about ten times more transmitter than the branch innervating the most proximal muscle fiber bundle (Meiss and Govind, 1979). Similarly, the lone inhibitory motor neuron

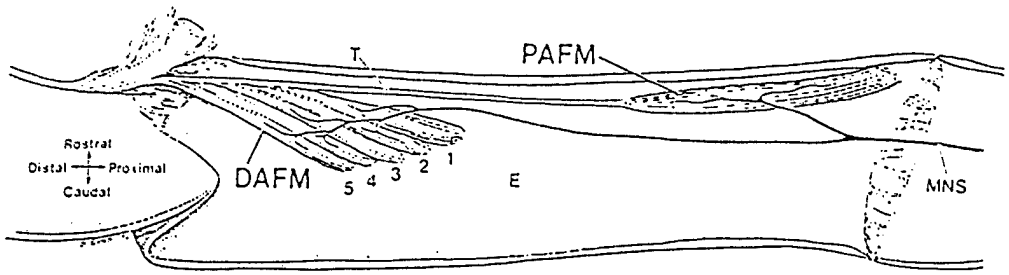

Figure 1. Illustration of the Proximal Accessory Flexor Muscle (PAFM) and the Distal Accessory Flexor Muscle (DAFM) in the lobster walking leg. Muscle fibers in the DAFM extend between a tendon (T) and the exoskeleton (E). One excitatory and one inhibitory motor neuron (MNS) innervate the DAFM. The DAFM is divided into five muscle fiber bundles: one proximal (1), three medial (2-4), and one distal (5). The excitor and inhibitor both release more transmitter onto the most distal muscle fiber bundle than onto the most proximal muscle fiber bundle. Adapted from Walrond, 1993.

innervating the DAFM releases about four to five times more transmitter on the most distal muscle fiber bundle than on the most proximal bundle (Walrond et al., 1990). The disparity in transmitter release in the excitor arises from differences in active zone structure (Walrond et al., 1993). In contrast, the difference in inhibitory synaptic strength appears to result from differences in active zone number since the terminal arborization is approximately five times larger on the distal muscle fiber bundle than on the proximal bundle (Walrond et al., 1993). Thus, the lobster provides a model of how two morphological variants may govern synaptic efficacy.

The lobster DAFM is a model particularly well-suited to appraise forms of neuronal remodeling because it can produce a quantifiable, experimentally induced modulation in synaptic efficacy. The distal accessory flexor muscle (DAFM) of the walking leg provides a convenient model for several reasons: 1) the DAFM is innervated by one excitatory (glutamatergic) and one inhibitory (GABAergic) motor neuron (Govind and Atwood, 1982), 2) synaptic efficacy can be estimated by intracellular recordings (Meiss and Govind, 1979), 3) increases in synaptic efficacy may be induced experimentally (Walrond, unpublished), 4) most of the synapses in the DAFM are located in varicosities that are readily identifiable in the light microscope (Walrond et al., 1993), and 5) the extent of innervation may be analyzed morphologically in the light microscope using *in vivo* labeling techniques.

Altering synaptic strength in the DAFM occurs by removing three or four of the eight walking legs and then allowing a recovery period of at least four weeks. Previous results (Walrond, unpublished) along with data from this study indicate that this paradigm leads to long-term increases in the amplitude of the excitatory postsynaptic potential

(EPSP). Because the muscle fiber input resistance remains unchanged in muscle fibers from experimental legs, the increase in EPSP amplitude appears to result from an increase in the amount of transmitter released. The experimentally-induced increase in the amount of transmitter released from the nerve terminal could result from alterations in three morphological parameters: active zone structure, an increase in active zone number in a relatively constant presynaptic area, and an increase in active zone number as a function of increased nerve terminal area. The question that this investigation addresses concerns changes in presynaptic area (i.e., increases in the extent of terminal arborization). Quantitative analysis using confocal light microscopy techniques and three-dimensional reconstructions of motor axon terminal arborizations permits the detection of changes in nerve terminal area. This investigation relies on these methods in determining if experimentally induced increases in synaptic efficacy are matched by increases in nerve terminal area.

MATERIALS AND METHODS

Lobster Preparation

Adult lobsters, ranging from 550 to 650 grams, were obtained from a local retailer and maintained at 13° C in two tanks containing artificial seawater. Each lobster was used to obtain control and experimental data. Four of the eight walking legs were removed and analyzed within a five day period to establish baseline data. Upon removal of the fourth leg, each lobster underwent an undisturbed recovery period of 28 days (minimum). After this time, the remaining four legs were removed and analyzed within a 5 day period to provide experimental data. All walking legs were removed and immersed in lobster physiological saline (472 mM NaCl, 10 mM KCl, 16 mM $CaCl_2$, 7 mM $MgCl_26H_2O$, 11 mM glucose, 10 mM Hepes) at pH 7.4 (Walrond et al. 1993). The DAFM was excised and mounted in 2 ml of saline for analysis in the light microscope.

Staining

This investigation used an activity-dependent dye, FM1-43 [N-(3-(triethyl ammonium) propyl)-4-(4-dibutylaminostyryl pyridinium) dibromide]. FM1-43 is an amphipathic fluorescent styryl dye that has been used in frog and *Drosophila* neuromuscular junctions and in rat hippocampal neurons to describe synaptic vesicle

cycling *in vivo* (Betz et al., 1992; Betz and Bewick, 1992, 1993; Ramaswami et al., 1994; Ryan, 1995). Incorporation into a lipid bilayer amplifies the dye's fluorescence about 200-fold. The short hydrophobic region of the molecule allows miscibility with one leaflet of the lipid bilayer while the hydrophilic region allows unbound dye to dilute into the aqueous medium (Ramaswami et al., 1994). Depolarizing the nerve terminal in the presence of dye causes transmitter release leading to the uptake of FM1-43 into synaptic vesicles via endocytosis. When extracellular dye is removed by washing, synapses remain labeled with dye that is trapped in the lumen of synaptic vesicles or in other endocytic organelles (VijayRaghavan, 1995; Ramaswami et al., 1994).

To load dye into the terminals, the DAFM was stimulated in a high K^+ saline (as described, except 432 mM NaCl and 50 mM KCl) in the presence of 2.5 μM FM1-43 for 15 minutes. The preparation was then repeatedly rinsed in physiological saline (as described, except 0 mM $CaCl_2$ and 23 mM $MgCl_26H_20$) to terminate vesicle recycling and wash away excess dye. Preparations show little or no reductions in fluorescence intensity while exposed to the low calcium/high potassium saline (data not shown). After bathing for 30 minutes in this solution, the preparation was transferred to the laser scanning confocal microscope for analysis.

Confocal Microscopy

Using a Sarastro 2000 confocal laser scanning fluorescence microscope linked to a Silicon Graphics 40G/30D three-dimensional image analysis system, fluorescent images were collected from both the dorsal and ventral sides of the most distal and most

proximal muscle fiber bundles. For each side of each muscle fiber bundle, a series of optical sections (75 scans at 4 μm intervals) was collected and reconstructed into a composite three-dimensional image. A Nikon PlanApo 10x/0.45 objective provided a balance between resolution and an adequate field of view. In addition, this objective provided sufficient working distance to permit reconstruction of the nerve terminal arborizations along the 300 μm z-axis. The laser was configured in a midrange setting to provide a clear image of all loaded terminals with minimal background "noise." Equipment settings were identical for all images (17.0 mW power setting, photomultiplier detector strength of 700, 10% attenuation, 510 beamsplitter, 535 long-pass filter, argon laser excitation of 10%, and a 100 μm aperture setting).

Imaging and Analysis

In this investigation, the term "image" refers to the three-dimensional reconstruction of 75 consecutive scans taken at 4 μm intervals on the confocal laser scanning microscope. Each image contained a segment of the distal or proximal muscle fiber bundle that was 1300 μm long. The image included the entire width of the muscle fiber bundle and covered approximately 15-20% of the length of each muscle fiber bundle. All images met the following criteria: a) the muscle fiber bundle was distinct from medial muscle fiber bundles, b) damaged fibers or the presence of connective tissue did not obstruct viewing of terminal arborizations, and c) the vertical axis of the three dimensional image encompassed all of the fluorescently labeled terminal arborizations acquired by the objective. Most images were of an area adjacent to the exoskeleton. This

method helped ensure that the same area of muscle was sampled for each preparation. In approximately 30% of the preparations, the viewing area next to the exoskeleton was marred by damaged muscle fibers or was obscured by connective tissue; in these cases, an image was acquired by moving the field of view toward the tendon until an undamaged, unobstructed area was found. Four images were obtained from each leg: one on each side of the distal bundle and one on each side of the proximal bundle.

To ensure data integrity, all raw images were transferred to a "write-once-read-many" compact disc using a Kodak PCD 2000 system. Measurements of the amount of innervation were obtained on a Gateway 2000 P5-133 computer with the Metamorph Imaging System (version 2.5). Because terminal arborizations were brightly labeled, the range of pixel intensity could be adjusted from the normal range of 0 (darkest) to 255 (brightest) to a range of 125 to 255; this thresholding allowed the elimination of weakly labeled muscle membrane and connective tissue but preserved labeled terminal arborizations for analysis. The result was an uncluttered preparation that distinctively displayed the pattern of innervation. Metamorph software calculated the ratio of the thresholded area to the planar area of the muscle fiber bundle to provide a value for the area covered by fluorescent axon terminals.

Images were categorized by animal and subcategorized based on type of leg (control or experimental) and type of muscle fiber bundle (distal or proximal). The control and experimental values for the area of muscle fiber bundle innervated were compared in each lobster using the Student's *t* test. For example, the images from the distal muscle fiber bundles of the four control legs belonging to lobster #1 were compared to the images from the distal muscle fiber bundles of the four experimental legs from

lobster #1. This method was repeated for images representing the proximal muscle fiber bundles. All three lobsters underwent the same analysis, and only "pair-wise" comparisons between control and experimental values within an individual lobster were made. Comparisons between animals were not utilized in order to avoid the statistical complications arising from animal-to-animal variability.

RESULTS

Staining and Imaging of Terminal Areas

The key to analyzing the nerve terminal arborization associated with the DAFM is the unambiguous identification of nerve terminals. FM1-43 is a nerve terminal specific dye which clearly labeled terminal areas on the DAFM (Fig. 2). This 40x image of a terminal arborization of the excitatory motor axon illustrates how the dye distinctly stained axonal branches and varicosities while producing minimal background labeling (Fig 2A). At the lobster neuromuscular synapse, FM1-43 appears to function through the vesicle recycling machinery. Stimulating FM1-43-labeled synapses caused brightly fluorescent, "loaded" terminals to lose fluorescence and become dimmer (Fig. 2B). The reduced fluorescence presumably results from exocytosis of dye-laden synaptic vesicles.

This investigation used 10x images of DAFM nerve terminal arborizations stained with FM1-43 to analyze the extent of neuronal innervation (Figure 3). Each image extended for 1300 μm along the length of the muscle fiber bundle, and encompassed the entire width. Depending on the size of the DAFM, the 1300 μm sample represents approximately 15 to 20% of the entire muscle fiber bundle length. Axon terminals were consistently and uniformly loaded with dye so that 89 of 96 images acquired from control and experimental animals in this study could be analyzed morphometrically. The seven unusable images resulted from damage sustained during

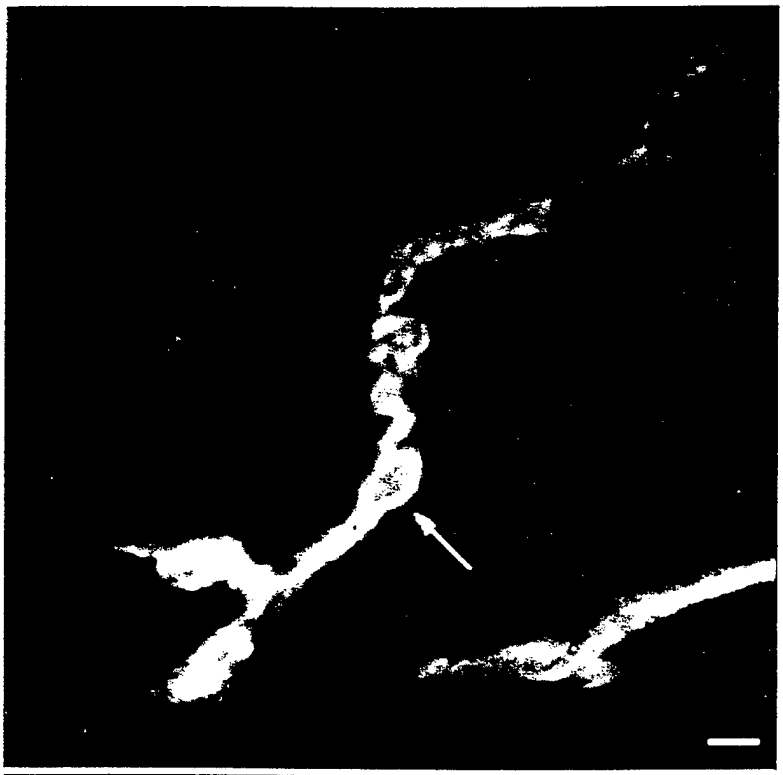

Figure 2A. Terminal arborization of an excitatory motor axon on the most distal muscle fiber bundle (40x). This preparation was loaded with 2.5 μM FM1-43 in high potassium (50mM) saline for 15 minutes. Most transmitter release is thought to occur from axonal swellings called varicosities (arrow). The large size of the varicosities indicates that this arborization is a branch of the excitatory motor neuron. Scale bar = 20 μm.

Figure 2B. Reduction of fluorescence in the terminal from 2A. Removing the dye and stimulating in 120 mM potassium reduced fluorescence in one varicosity by 40% (arrow). Overall, the stimulation reduced fluorescence by 45%. Scale bar = 20μm.

Figure 2. Excitatory nerve terminal varicosities on a DAFM distal muscle fiber bundle loaded with FM1-43 and subsequently unloaded.

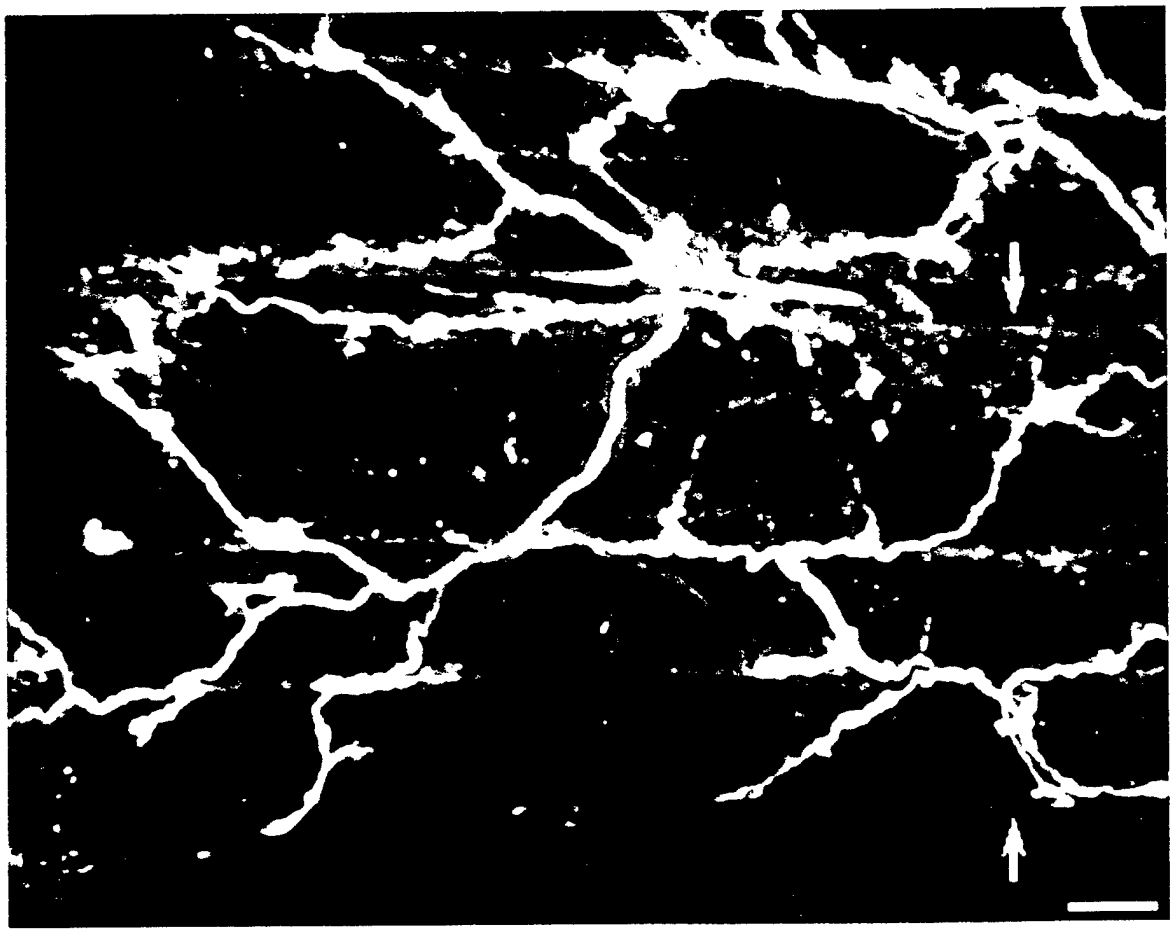

Figure 3. A typical 10x image of nerve terminal arborizations stained with FM1-43 on a DAFM proximal muscle fiber bundle. The terminal arborization shows the pattern of innervation in the proximal muscle fiber bundle. The preparation was stained with FM1-43 and images of the nerve terminal were reconstructed from 75 consecutive scans collected at 4 μm intervals along the vertical (z) axis. The length of the muscle fiber bundle scanned in these images is 1300 μm and represents 15 to 20% of the length of the bundle. The width of the proximal muscle fiber bundle is indicated by the white arrows.
Scale bar = 100 μm.

dissection or obstruction of nerve terminal views caused by connective tissue. Overall, using FM1-43 in combination with confocal laser scanning fluorescence microscopy provided a sound methodology for quantifying the extent of innervation in the DAFM.

Measurements of Synaptic Efficacy

To establish control values for synaptic efficacy in distal and proximal muscle fiber bundles, a series of electrophysiological measurements were made (all electrophysiological analysis was performed by Scott Druecker). Baseline data was provided by measuring EPSP amplitudes in 21 distal accessory flexor muscles from seven lobsters (unpublished data). In these control experiments, measurements were made in 71 distal and 72 proximal muscle fibers. The EPSP amplitudes averaged 6.42 ± .46 mV (SEM) distally, and 0.37 ± .04 mV proximally. To ensure that leg removal had increased synaptic efficacy in the present study, EPSP's were measured in proximal and distal muscle fiber bundles in five muscles from experimental legs in two animals. In the experimental muscles, the mean EPSP amplitude recorded distally was 11.68 ± 1.2 mV and the mean amplitude recorded proximally was 1.49 ± .22 mV. These changes represent increases in EPSP amplitude of 303% and 82% for the proximal and distal muscle fiber bundles, respectively.

The experimental measurements from two lobsters used in this study were compared with a library of control measurements of EPSP amplitude obtained from similar lobsters in previous investigations. The distribution of EPSP amplitudes for both the proximal and the distal muscle fiber bundles in experimental animals were shifted

toward larger values (Figs. 4 and 5). For the distal bundle, EPSP amplitudes averaged 6.42 mV for controls and 11.68 mV for experimental preparations. For the proximal bundle, the average EPSP amplitude was 0.37 mV for controls 1.49 mV for experimental preparations. These data affirm that leg removal followed by a waiting period produced a significant increase in proximal and distal EPSP amplitude ($p<.01$, Student's *t* test). As compared to controls, EPSP amplitude in the distal fibers showed a smaller proportional increase (82%) than in the proximal fibers. However, the 5 mV increase in EPSP amplitude represents a great increase in the number of quanta released than the 1 mV increase observed in the proximal muscle fiber bundle.

The histogram showing EPSP amplitudes from control and experimental proximal muscle fiber bundles illustrates the experimentally induced increase in synaptic strength (Fig. 5). Almost 80% of the EPSP amplitudes were 0.4 mV or less in the proximal muscle fiber bundles from control legs. In contrast, 75% of the EPSP recordings from experimental legs were greater than 0.8 mV. Overall, mean EPSP amplitudes from the proximal muscle fiber bundles of experimental legs showed an increase of 303% over the values recorded in control legs.

These findings were in agreement with earlier studies which compared EPSP amplitudes in the same animal before and after leg removal. These studies showed increasing EPSP amplitudes of 77% distally and 260% proximally (Walrond and Druecker, unpublished). Because neither the changes in the earlier studies nor in the present study were accompanied by changes in the muscle fiber input resistance, the increase in EPSP amplitude likely resulted from increases in the amount of transmitter released. One mechanism to accommodate the observed increases in the amount of

transmitter released in the DAFM would be to increase the extent of the nerve terminal arborizations. Determining if such alterations in nerve terminal structure accompany the physiological changes is the main focus of this investigation.

Measurements of Neuronal Innervation

Control values for the extent of neuronal innervation of distal and proximal muscle fiber bundles were provided by the four control legs in each lobster, and experimental values were obtained from the remaining four legs from the same animal. Table 1 lists these values as the proportion of muscle fiber surface area covered by stained motor axon terminal. The number of legs is shown in parentheses and the number of reconstructions is shown in brackets.

	PROXIMAL			DISTAL		
LOBSTER	CONTROL	EXPMT	P-VALUE	CONTROL	EXPMT	P-VALUE
1	6.31 ± .87 (4)[8]	6.76 ± .70 (4)[8]	.69	6.03 ± .80 (4)[8]	5.59 ± .98 (4)[8]	.72
2	5.19 ± .75 (2)[4]	4.94 ± .91 (4)[8]	.86	6.45 ± .38 (3)[6]	6.58 ± .60 (4)[8]	.87
3	6.42 ± .76 (4)[8]	6.17 ± .80 (4)[8]	.83	7.82 ± .81 (4)[8]	9.40 ± .86 (4)[7]	.20

Table 1. Comparison of the area of muscle fiber surface occupied by fluorescently labeled axon terminals in control and experimental legs from three animals. The area of muscle fiber occupied by axon terminal is expressed as a percent of the surface area of the muscle fiber bundle occupied by fluorescently labeled axon terminal. The table is subdivided into control and experimental columns for proximal and distal muscle fiber bundles. The P-value is derived from a student's *t*-test and represents a comparison of the control and experimental values. For each lobster, an increase in synaptic efficacy was not accompanied by a significant increase in neuronal innervation in distal or proximal muscle fiber bundles ($p > .05$). Depicted values indicate the mean percentage of neuronal innervation ± SEM in ( ) legs and [ ] images per lobster.

In each animal, the change in the area of muscle fiber surface area occupied by fluorescently labeled nerve terminal in control and experimental legs was not significant in any case. For example, the mean area occupied by nerve terminal in the proximal muscle fiber bundle from animal #1 was 6.31%, and the experimental value was 6.76%. This difference represented the largest increase for values from the proximal bundle in any of the lobsters, but a P-value of 0.69 indicated that the change was not significant. The remaining proximal comparisons show that the 303% increase in EPSP amplitude was not accompanied by an equivalent increase in the motor axon terminal area. Similarly, the 82% increase in distal EPSP amplitude was not accompanied by a significant alteration of nerve terminal area on distal muscle fiber bundles. Although one animal showed an apparent increase in the mean percentage of neuronal innervation (7.82% to 9.40%), the statistical comparison showed a P-value of 0.20. The P-values for the distal muscle fiber bundle comparisons in the other two animals were much higher and indicated that experimentally induced increases in EPSP amplitude cause little or no increase in synaptic area. Taken individually and in total, these measurements indicated that an increase in synaptic efficacy was not accompanied by a significant change in the area of muscle fiber occupied by nerve terminal arborization.

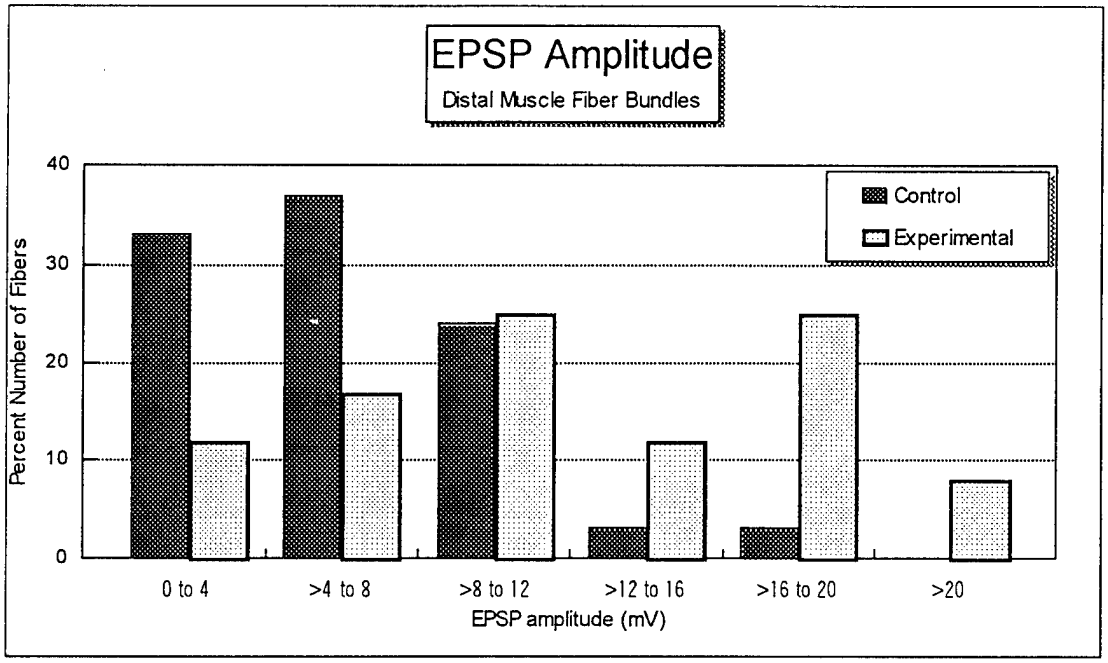

FIGURE 4. Frequency histogram comparing synaptic efficacy in control and experimental distal muscle fiber bundles. 71 control measurements from seven lobsters and 24 experimental measurements from two lobsters are presented. The abscissa represents the EPSP amplitude (in mV) measured from individual muscle fibers. The ordinate represents the proportion (as a percentage of total measurements) from muscle fibers in each range of EPSP values depicted on the abscissa. This histogram shows a rightward shift for the experimental muscle fiber measurements, indicating an 82% increase in synaptic efficacy for these muscle fibers.

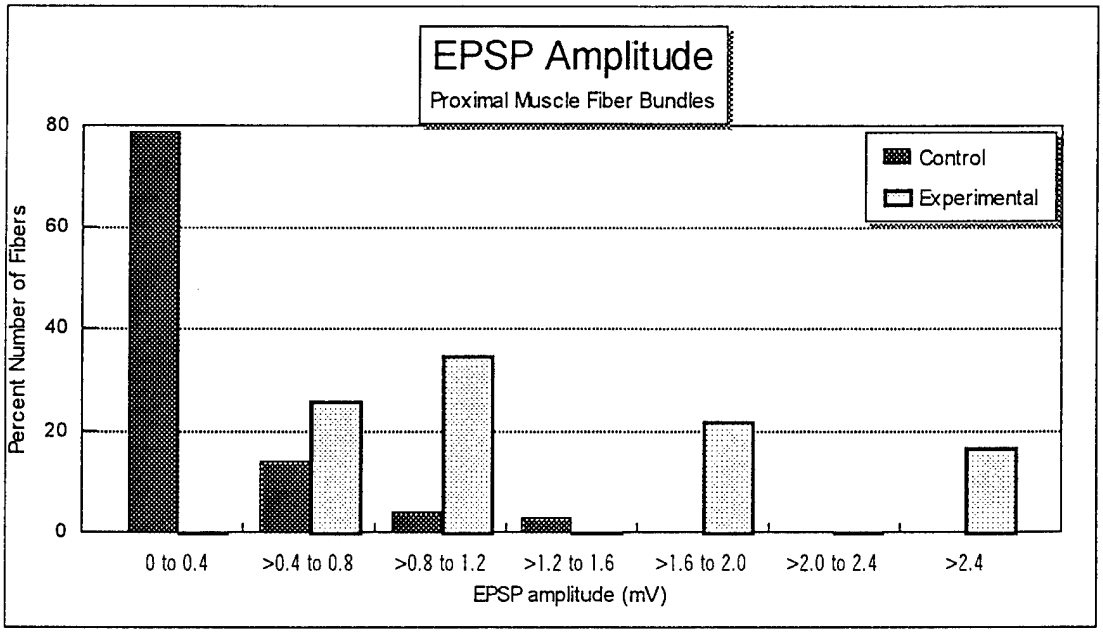

FIGURE 5. Frequency histogram comparing synaptic efficacy in control and experimental proximal muscle fiber bundles. 72 control measurements from seven lobsters and 24 experimental measurements from two lobsters are presented. The abscissa represents the EPSP amplitude (ranging from 0 to >2.4 mV) measured from individual muscle fibers. The ordinate represents the number of measurements (as a percentage of total measurements) from individual muscle fibers. The majority of control values range from 0 to 0.4 mV, whereas the experimental values show a marked increase. The histogram represents a 303% overall increase in synaptic efficacy between control and experimental legs.

DISCUSSION

Overview of Findings

Electrophysiological analysis of EPSP amplitudes in muscles from experimental legs reaffirms that increases in synaptic efficacy are inducible in the lobster DAFM. This study examines the correlation between the change in synaptic strength and presynaptic morphological alterations. The results show that muscle fiber surface area occupied by nerve terminals is similar in images from control and experimental muscles in both the distal and proximal muscle fiber bundles. Therefore, it is unlikely that increased synaptic efficacy relies exclusively on changes in nerve terminal arborization.

In the DAFM, neurotransmitter release is regionally differentiated such that the single inhibitory and excitatory motor neurons both release more transmitter on the most distal muscle fiber bundle than on the most proximal muscle fiber bundle. The proximal-distal disparity in synaptic strength is 4-5 fold for the inhibitor and 10 fold for the excitor (Meiss and Govind, 1979; Walrond et al., 1990). The difference in synaptic strength observed with the inhibitor is associated with a four fold increase in the size of the terminal arborization on the distal muscle fiber bundle (Walrond et al., 1990; Walrond et al., 1993). The correspondence between the size of the arbor and synaptic strength suggests that the formation of additional branches via axonal sprouting could produce an

increase in synaptic efficacy. However, pair-wise comparisons between control and experimental values indicate that alterations in the size of the axon terminal arborization cannot account for the observed increase in synaptic efficacy (Table 1). Nevertheless, we cannot rule out a small contribution to the increase in synaptic efficacy through a modest experimentally induced increase in the extent of terminal arborization that is masked by variation among muscles from the same animal and/or by minor inconsistencies in measurement. In earlier studies, the number of excitatory synapses on the proximal and distal muscle fiber bundles was compared by cutting thin sections at regular intervals along the length of the muscle and counting the number of synapses at each station (Walrond et al., 1993). The proximal-distal disparity in synapse number was insufficient to account for the disparity in synaptic efficacy. The present study confirms and extends these observations by showing that the muscle fiber area occupied by the axon terminal is similar for proximal and distal bundles.

Although changes in the size of the excitatory nerve terminal arborization could contribute to increases in synaptic efficacy, the results of this investigation indicate that sprouting is not the sole factor. If growth in the terminal arborization promotes the increase in synaptic efficacy, then this increase occurs in concert with other forms of structural remodeling such as changes in the size of varicosities or alterations in active zone number or structure.

Alternative Forms of Synaptic Remodeling

Presynaptic structural remodeling. Although enhanced synaptic efficacy does not appear to result solely from the sprouting of new axon terminals, other morphological alterations could account for an increase in active zone number. For example, increasing the size of varicosities to accommodate more synapses and therefore more active zones is a plausible alternative (Yeow and Peterson, 1991). Varicosity size directly correlates with active zone number and area; it is also a good predictor of synaptic strength in a variety of species and brain regions, including frog cardiac ganglia, rat visual cortex, cat lateral geniculate nucleus, turtle and cat spinal cord, and rat cerebellar cortex and hippocampus (for a review, see Pierce and Lewin, 1994). Comparison of varicosity sizes can be readily made in the DAFM using the light microscope. Because this study focused on alterations in the size of the terminal arborization, large fields of view were used to maximize the surface area of muscle sampled. As a consequence, the magnification used was too low to resolve subtle changes in varicosity size. However, increases in varicosity size sufficient to account entirely for the 303% increase in transmitter release in the proximal muscle fiber bundle would likely have been observed as an increase in nerve terminal area. Since nerve terminal area remains nearly constant in experimental preparations, increases in synaptic efficacy may result largely from changes in synapse structure within a constant area of motor axon terminal.

In the DAFM, the excitatory neuron appears to mediate differences in transmitter release between the proximal and distal muscle fiber bundles via a difference in active zone structure (Walrond et al., 1993). This suggests that experimentally induced changes

in synaptic efficacy might be closely related to structural changes in active zones and not necessarily to changes in active zone number. Increases in synaptic efficacy have been associated with structural changes at active zones in other systems, such as *Aplysia* sensory to motor neuron synapses and the frog neuromuscular junction. Since it is improbable that experimentally induced changes in synaptic strength in the DAFM rely strictly on an increase in the size of the terminal arborization, one (or both) of these alternative mechanisms—increasing active zone number or altering active zone structure without the addition of new axonal terminals —is likely to play a key role in synaptic plasticity at the lobster neuromuscular junction.

Postsynaptic Remodeling. In arthropods, the postsynaptic membranes of excitatory neuromuscular synapses are identified in freeze-fractured preparations as circular or oval patches of tightly packed E-face particles (Franzini-Armstrong, 1976; Rheuben, 1985; Walrond et al., 1993). In *Drosophila* and lobster, the patches are 0.2 to 0.3 μm^2 and the particles are thought to represent glutamate receptors (Walrond et al., 1993; Stewart et al., 1996). Mutations that increase postsynaptic areas by two to three fold in *Drosophila* lead to about a 20% increase in the amplitude of the unitary quantal event (Stewart et al., 1996). It is unclear if similar factors contribute to the experimentally induced increases in EPSP amplitude observed in lobster, but it will be important to consider the possible effects of postsynaptic structural modifications in long-term changes in synaptic efficacy in the lobster DAFM.

Considerations Involving Light Microscopy

Selecting the appropriate magnification. The 10x objective reliably samples the degree of innervation present on the proximal and distal muscle fiber bundles of the DAFM. Each image represents approximately 10% to 25% of the length of the entire bundle, and encompasses the full width of the bundle (Fig. 3). Using previously described staining procedures, the pattern of innervation appeared to be similar throughout the length of the proximal and distal muscle fiber bundles (Fig. 6), and most images were of an area adjacent to the exoskeleton. Selecting this region helped ensure continuity from sample to sample and minimized the subjective bias involved with searching for the most heavily innervated segment. In some cases, an area farther from the exoskeleton was imaged because of damage or the interference of connective tissue. Because the pattern of innervation does not appear to vary with muscle region, these images provide an accurate representation of the extent of innervation.

The disadvantage of imaging a large section of each muscle fiber bundle is limited resolution. The 10x objective is appropriate for this study since compromise between resolution and field of view permitted an account of axonal sprouting or elongation of terminal arborizations. This magnification easily revealed the terminal arborizations, and individual varicosities were sometimes discernible along the axonal branches (Figure 3). However, a change in the size of varicosities or in their number along a fixed branch length would be difficult to quantify at this magnification. If increases in active zone number are accomplished by enlarging the varicosities, higher magnification (20x or 40x) with a higher numerical aperture will be necessary to quantify these changes (Fig. 7).

Figure 6. Innervation along 95% of a distal muscle fiber bundle stained with FM1-43. Connections to the exoskeleton (far left) and to the tendon (far right) are not shown. A portion of the bundle is occluded from view by nerve (arrowheads). The pattern of innervation appears to be similar along the length of the muscle fiber bundle. Most images analyzed in this study were taken from the 1300 μm long area closest to the exoskeleton.
Scale bar = 500 μm.

Figure 7A. A 10x view of nerve terminals loaded with FM1-43 on a proximal muscle fiber bundle. The pattern of innervation is clear, but individual varicosities are difficult to discern and measure at this magnification. The portion on the lower left is enlarged in 7B and 7C.
Scale bar = 200 μm.

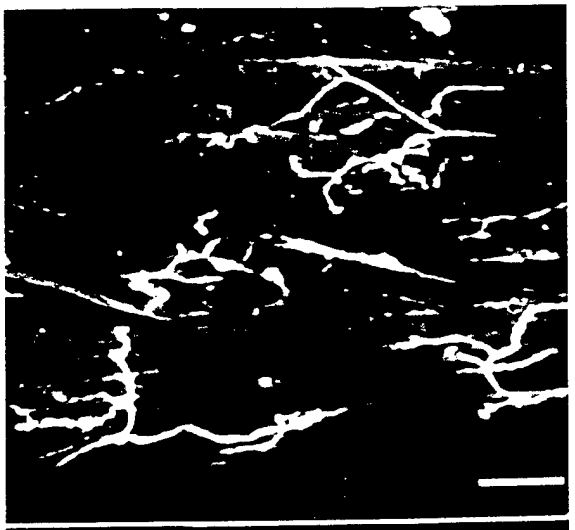

Figure 7B. A 20x view of a region shown in 7A. Here, varicosities are discernible but the image samples only a small portion of the muscle fiber bundle.
Scale bar = 100 μm.

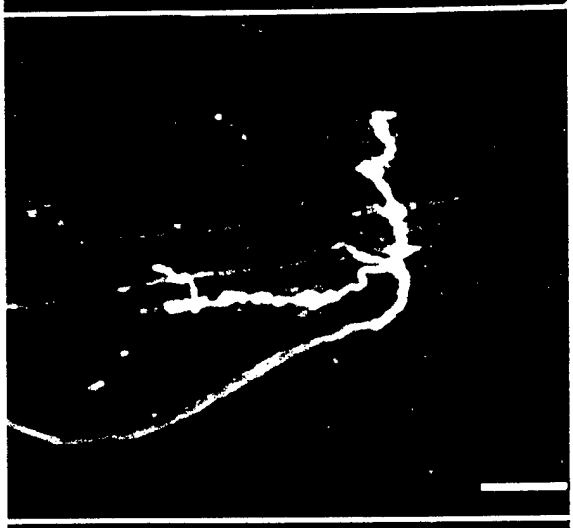

Figure 7C. This 40x image of the same area as 7B provides a much sharper illustration of varicosities. Significant changes in varicosity size would be quantifiable at this magnification, but only a very small portion of the entire muscle fiber bundle is visible.
Scale bar = 50 μm.

Figure 7. Comparison of a nerve terminal area on a proximal fiber bundle at increasing magnification.

Although increased resolution has its advantages, it comes at the expense of examining only a limited section of the entire muscle fiber bundle. Overcoming this disadvantage would require obtaining many more images of control and experimental preparations to avoid bias and to ensure the whole muscle fiber bundle is adequately represented.

In the distal muscle fiber bundle, the terminal arborization of the inhibitor and excitor are usually located near one another (Walrond et al., 1990). However, the two can be distinguished in the light microscope based on morphological differences. Inhibitory varicosities on average measure only 3.0 μm and 1.9 μm along the major and minor axis, respectively (Walrond et al., 1993). In contrast, excitatory varicosities are considerably larger, and may exceed 20 μm along the major axis and 10 μm along the minor axis. The axonal connections between the inhibitory varicosities are about 1 μm in diameter whereas the processes connecting excitatory varicosities are larger than 3 μm in diameter. Although it is likely that both the excitor and inhibitor are stimulated strongly enough to take up FM1-43, the pattern of inhibitory innervation was not obvious. It is unclear if the resolution of these studies was sufficient to distinguish between the excitor and inhibitor or if the inhibitor took up less dye. Staining the preparation with antibodies to the inhibitory neurotransmitter (GABA) following experiments with FM1-43 may distinguish between these possibilities. These studies could allow inhibitory nerve terminal morphology to be quantified independently of the excitor.

Constructing a three-dimensional image. A three-dimensional, 300 μm deep image maximizes the amount of presynaptic terminal visible in a muscle fiber bundle.

Some regions of the terminal are on the surface while others may not become visible until 30 or 40 scans into the preparation. There seems to be little loss of resolution in the three-dimensional reconstructions of the first 200 μm, and terminal regions are frequently separated by more than 150 μm along the z-axis. In some cases, terminal areas are not visible within the first 100 μm of the surface of the muscle fiber bundle (Fig. 8). Nevertheless, the resolution in these three-dimensional images falls of within the depth of the muscle fiber bundle since scans could not be made through the entire thickness of the muscle fiber bundle. To help obviate this problem, scans were made on the dorsal and ventral surface of each muscle fiber bundle.

Another concern involves the possible loss of information with the 4 μm step size. Smaller varicosities such as those associated with the inhibitor measure about 3.0 μm by 1.9 μm (Walrond et al., 1993). These structures could fall between two scans and not contribute to the fluorescence image of the terminal arborization. To investigate the possible shortcomings of the large step size, the same three-dimensional area was scanned at 0.9 μm and 4.0 μm step sizes (Fig. 9). The image reconstructed from the smaller step size provides a more detailed account of stained structures, but muscle area occupied was virtually the same regardless of step size (4.47% and 4.44%, respectively).

Future Directions

Light microscopy. Since a significant increase in the degree of terminal arborization does not accompany increases in synaptic efficacy, presynaptic structural remodeling may occur on a smaller scale. It appears unlikely that the number of

Figure 8A. Reconstruction (75 sections, 4 μm step size) of a nerve terminal arborization loaded with FM1-43 on a proximal muscle fiber bundle. About 7.75% of the muscle fiber surface area is occupied by labeled nerve terminal Scale bar = 100 μm (10x)

Figure 8B. The first 25 sections (0-100 μm) of 8A. Many terminal areas are not yet visible in the lower third of this image. The labeled terminals occupy 5.33% of the planar area of the muscle fiber bundle. Scale bar = 100 μm (10x)

Figure 8C. The middle 25 sections (100-200 μm) of 8A. Terminal areas not seen in 8B are now visible. The labeled terminals occupy 4.61% of the planar area of the muscle fiber bundle. Scale bar = 100 μm (10x)

Figure 8D. The last 25 sections (200-300 μm) of 8A. Most of the terminals visible here are also in 8C, indicating that resolution has declined or innervation does not penetrate this deeply into the muscle fiber bundle. Fluorescently labeled terminals occupy only 0.53% of the planar area of the muscle fiber bundle. Scale bar = 100 μm (10x)

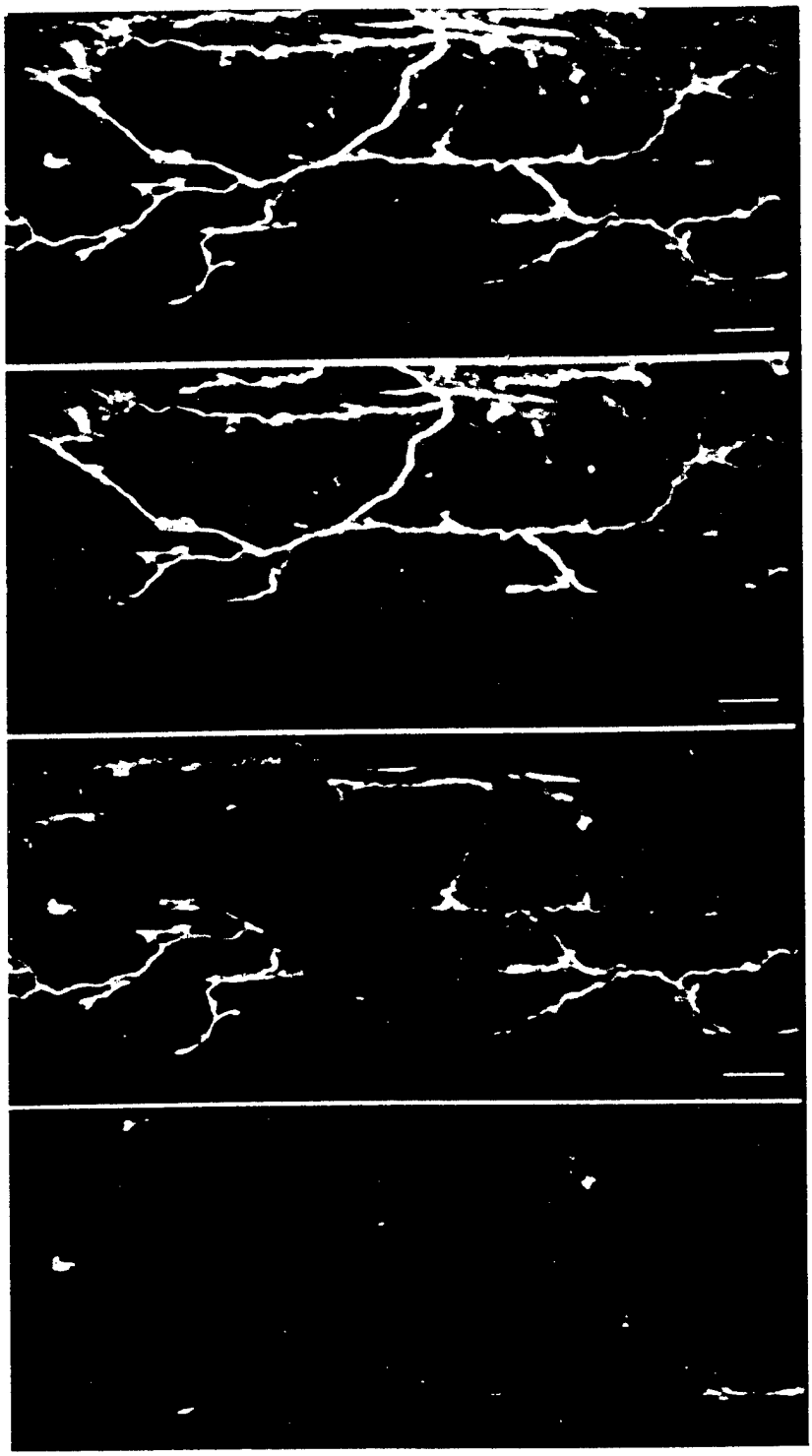

Figure 8. Optical sections from three levels in a single 3-D reconstruction

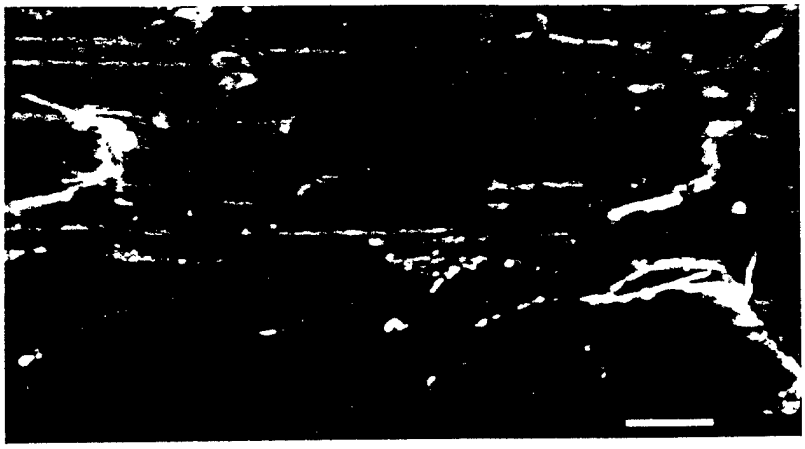

Figure 9A. A portion of the innervation on a distal muscle fiber bundle stained with FM1-43. 14 scans at 4 μm sequential intervals were combined to make this 56 μm thick image. Smaller terminal areas may be represented by only one or two scans. The area occupied by innervation is 4.44%.
Scale bar = 100 μm (10x)

Figure 9B. The same region as 9A reconstructed from 60 individual scans taken at sequential 0.9 μm intervals. The terminal areas are brighter than in 9A, but the pattern and area occupied by innervation (4.47%) are unaffected.
Scale bar = 100 μm (10x)

Figure 9. Reducing the step size has little effect on measurements of muscle fiber area occupied by nerve terminal in 10x views.

varicosities increases through the addition of new axonal branches, but varicosities might enlarge or their number per length of axon terminal may increase within a fixed size of the terminal arborization. Such changes could be visualized by using higher magnification/N.A. objectives (Fig. 7). At higher magnification, a sampling method adequately representing the entire muscle will need to be developed. One drawback to these studies is the large number of images that will be required to provide an adequate sample size. An alternate technique for studying the number and distribution of varicosities may be to use a synaptotagmin antibody to label varicosities in the axon terminal. Terminals labeled in this way will be easily visualized and their dimensions quantified in the light microscope.

Electron microscopy. Ultimately, electron microscopy will be required to relate experimentally induced increases in synaptic efficacy with alterations in synaptic structure. A combination of studies using serial thin sectioning and freeze-fracture will be employed to determine if changes in a postsynaptic area, active zone number per synapse, and/or active zone structure can account for the increase in synaptic efficacy. Several of the DAFMs used in this investigation have been prepared for this type of analysis.

Conclusion

This investigation completes the first step in determining how synaptic plasticity and synaptic efficacy are functionally related in the lobster neuromuscular junction. One

possible form of structural remodeling that may accommodate changes in synaptic efficacy is an increase in the size of the nerve terminal arborization. The use of confocal laser scanning fluorescence microscopy and a nerve terminal specific dye shows that lobsters demonstrating a significant increase in synaptic efficacy do not display commensurate changes in the degree of neuronal innervation such as axonal sprouting or elongation of terminal arborizations. Therefore, alterations in the extent of nerve terminal arborization in the DAFM of *Homarus americanus* cannot account for an experimentally induced increase in synaptic efficacy. This suggests that increased synaptic efficacy may instead result from structural changes at the level of the synapse and/or active zone.

REFERENCES CITED

Adler EM, Augustine GJ, Duffy SN, Charlton MP (1991) Alien intracellular calcium chelators attenuate neurotransmitter release at the squid giant synapse. Journal of Neuroscience 11:1496-1507.

Atwood HL, Marin L (1983) Ultrastructure of synapses with different transmitter-releasing characteristics on motor axon terminals of a crab, *Hyas areneas*. Cell Tissue Res. 231:103-115.

Atwood HL, Cooper RL, Wojtowicz JM (1994) Nonuniformity and plasticity of quantal release at crustacean motor nerve terminals. Molecular and Cellular Mechanisms of Neurotransmitter Release. Raven Press, NY.

Augustine GJ, Charlton MP, Smith SJ (1985) Calcium entry and transmitter release at voltage-clamped nerve terminals of squid. J. Physiol. (Lond.) 367:163-181

Bailey CH, Chen M (1983) Morphological basis of long-term habituation and sensitization in *Aplysia*. Science 220:91-93.

Bailey CH, Chen M (1988) Long-term memory in *Aplysia* modulates the total number of varicosities of single identified sensory neurons. Proc. Natl. Acad. Sci. (USA) 85:2372-77.

Bailey CH, Chen M (1988) Long-term sensitization in *Aplysia* increases the number of presynaptic contacts onto the identified gill motor neuron L7. Proc. Natl. Acad. Sci. (USA) 85:9356-5939.

Bailey CH, Chen M (1989) Structural plasticity at identified synapses during long-term memory in *Aplysia*. Journal of Neurobiology 20:356-372.

Bailey CH, Kandel ER (1993) Structural changes accompanying memory storage. Annu. Rev. Physiol. 55:397-426.

Betz WJ, Bewick GS (1992) Optical analysis of synaptic vesicle recycling at the frog neuromuscular junction. Science 255:200-203.

Betz WJ, Mao F, Bewick GS (1992) Activity-dependent fluorescent staining and destaining of living motor nerve terminals. Journal of Neuroscience 12:363-375.

Betz WJ, Bewick GS (1993) Optical monitoring of transmitter release and synaptic vesicle recycling at the frog neuromuscular junction. Journal of Physiology 460:287-309.

Brown MC, Ironton R (1977) Motoneurone sprouting induced by prolonged tetrodotoxin block of nerve action potential. Nature 265:459-461.

Brown MC, Holland RL, Hopkins WG (1981) Motor Nerve Sprouting. Annu Rev. Neurosci. 4:17-42.

Budnik V, Zhong y, Wu C (1990) Morphological plasticity of motor axons in Drosophila mutants with altered excitability. Journal of Neuroscience 10(11):3754-3768

Cooper RL, Marin L, Atwood HL (1995) Synaptic differentiation of a single motor neuron: conjoint definition of transmitter release, presynaptic calcium signals, and ultrastructure. Journal of Neuroscience 15(6):4209-4222.

Couteaux R, Pecot-Dechavassine M (1970) Vesicules synaptiques et poches au niveau des zones actives de la jonction neuromusculaire. Compt Rend Acad Sci (Paris) 271:2346-2349.

Del Castillo J, Katz B (1954) Statistical factors involved in neuromuscular facilitation and depression. J. Physiol. (Lond.) 124:574.

Desmond NL, Levy WB (1988) Synaptic interface surface area increases with long-term potentiation in the hippocampal dentate gyrus. Brain Research 453:308-314.

Dodge and Rahamimoff (1967) Cooperative action of calcium ions in transmitter release at the neuromuscular junction. J. Physiol. (Lond.) 193:419-432.

Dryer F, Peper K, Akert K, Sandri C, Moor H (1973) Ultrastructure of the "active zone" in the frog neuromuscular junction. Brain Research 62:373-380.

Fatt P, Katz B (1952) Spontaneous threshold activity at motor nerve endings. J. Physiol. (Lond.) 117:109-128.

Florey E, Cahill MA (1982) The innervation pattern of crustacean skeletal muscle. Cell Tissue Research 224:527-541.

Franzini-Armstrong C (1976) Freeze-fracture of excitatory and inhibitory synapses in crayfish neuromuscular junctions. J. Micros. Biol. Cell 25:217-229.

Fukunaga H, Engel AG, Lang B, Newsom-Davis J, Vincent A (1983) Passive transfer of the Lambert-Eaton myasthenic syndrome with IgG from man to mouse depletes the presynaptic active zones. Proc. Natl. Acad. Sci (USA) 80:7636-7640.

Garcia KD, Mynlieff M, Sanders DB, Beam KG, Walrond JP (1996) Lambert-Eaton sera reduce low-voltage and high-voltage activated calcium currents in murine dorsal root ganglion neurons. Proc. Natl. Acad. Sci (USA) 93:9264-9269.

Govind CK, Chiang RG (1979) Correlation between presynaptic dense bodies and transmitter output at lobster neuromuscular terminals by serial section electron microscopy. Brain Research 161:377-388.

Govind CK, Meiss DE (1979) Quantitative comparison of low and high-output neuromuscular synapses from a motoneuron of the lobster (*Homarus americanus*). Cell Tiss. Res. 198:455-463.

Govind CK, Atwood HL (1982) Organization of neuromuscular systems. The Biology of Crustacea., Vol 3 Neurobiology: Structure and Function. DE BLiss, HL Atwood, DC Sandeman, Eds. (Academic Press, New York).

Govind CK, Pearce J (1982) Proliferation and relocation of developing lobster neuromuscular synapses. Developmental Biology 90:67-78.

Gulley RL, Landis DMD, Reese TS (1978) Internal organization of membranes and end bulbs of Held in the anteroventral cochlear nucleus. J Comp Neurol 180:707-742.

Herrera AA, Grinnel AD (1981) Contralateral denervation causes enhanced transmitter release from frog motor nerve terminals. Nature 291:495-497.

Herrera AA, Grinnel AD, Wolowske B (1985) Ultrastructural correlates of experimentally altered transmitter release efficacy in frog motor nerve terminals. Neuroscience.

Heuser JE, Reese TS (1973) Evidence for recycling of synaptic vesicle membrane during transmitter release at the frog neuromuscular junction. Journal of Cell Biology 57:315-344.

Heuser JE, Reese TS, Landis DMD (1974) Functional changes in frog neuromuscular junctions studied with freeze-fracture. Journal of Neurocytology 3:109-131.

Heuser JE, Reese TS, Dennis MJ, Jan Y, Jan L, Evans L (1979) Synaptic vesicle exocytosis captured by quick freezing and correlated with quantal transmitter release. Journal of Cell Biology 81:275-300.

Katz B (1962) The transmission of impulses from nerve to muscle, and the subcellular unit of synaptic action. Proc. R. Soc. Lond. B Biol. Sci. 155:455

Katz B (1966) Nerve, Muscle, and Synapse. Mcgraw-Hill, New York.

Katz B, Miledi R (1967) The timing of calcium action during neuromuscular transmission. J. Physiol. (Lond.) 189:534-544.

Katz B (1969) The release of neural transmitter substances. Liverpool University Press, Liverpool.

Llinas R, Steinberg IZ, Walton K (1981) Relationship between presynaptic calcium current and postsynaptic potential in squid giant synapse. Biophys J 33:323-351.

Lnenicka GA, Atwood HL, Marin L (1986) Morphological transformation of synaptic terminals of a phasic motoneuron by long-term tonic stimulation. Journal of Neuroscience 6(8):2252-2258.

Lnenicka GA, Hong SJ (1988) Activity-dependent development of synaptic varicosities at crayfish motor terminals. Journal of Neuroscience 11:1040-1048.

Meiss DE, Govind CK (1979) Multiterminal innervation: non-uniform density along single lobster muscle fibers. Brain Research 160:163-169.

Meiss DE, Govind CK (1980) Heterogeneity of existing synapses at the ends of single muscle fibers in the lobster, *Homarus americanus*. Journal of Neurobiology 11:381-395.

Pearce J, Govind CK, Meiss DE (1985) Growth-related features of lobster neuromuscular terminals. Developmental Brain Research 21:215-228.

Pearce J, Govind CK, Shivers R (1986) Intramembranous organization of lobster excitatory neuromuscular synapses. Journal of Neurocytology 15:241-252.

Pierce JP, Lewin GR (1994) An ultrastructural size principle. Neuroscience 58(3):441-446.

Propst JW, Ko C (1987) Correlations between active zone ultrastructure and synaptic function studied with freeze-fracture of physiologically indentified neuromuscular junctions. Journal of Neuroscience 7(11):3654-3664.

Pumplin DW, Reese TS, Llinas R (1981) Are the presynaptic active zone particles the calcium channels? Proc. Natl. Acad. Sci (USA) 78:7210-7214.

Ramaswami M, Krishnan KS, Kelly RB (1994) Intermediates in synaptic vesicle recycling revealed by optical imaging of Drosophila neuromuscular junctions. Neuron 13:363-375.

Rash JE, Walrond JP, Morita M (1988) Structural and functional correlates of synaptic transmission in the vertebrate neuromuscular junction. Journal of Electron Microscopy 10:153-185.

Rheuben MB (1985) Quantitative comparison of the structural features of slow and fast neuromuscular junctions in *Manduca*. Journal of Neuroscience 5:1704-1716.

Roberts WM, Jacobs RA, Hudspeth AJ (1990) Colocalization of ion channels involved in frequency selectivity and synaptic transmission at presynaptic active zones of hair cells. Journal of Neuroscience 10:3664-3684.

Ryan TA, Smith SJ (1995) Vesicle pool mobilization during action potential firing at hippocampal synapses. Neuron 14:983-989.

Stewart BA, Schuster CM, Goodman CS, Atwood HL (1996) Homeostasis of synaptic transmission in *Drosophila* with genetically altered nerve terminal morphology. Journal of Neuroscience 16(12):3877-3886.

VijayRaghavan K (1995) Synaptic vesicle recycling intermediates revealed. BioEssays 17:195-198.

Walrond JW, Reese TS (1985) Structure of axon terminals and active zones at synapses on lizard twitch and tonic muscle fibers. Journal of Neuroscience 5:1118-1131.

Walrond JP, Govind CK, Heustis SE (1993) Two Structural adaptations for regulating transmitter release at lobster neuromuscular synapses. Journal of Neuroscience 11:4831-4845.

Wernig A, Herrera AA (1986) Sprouting and remodeling at the nerve muscle junction. Progress in Neurobiology 27:251-291.

Yeow MBL, Peterson EH (1991) Active zone organization and vesicle content scale with bouton size at a vertebrate central synapse. J. Comp. Neurol. 307:475-586.

Zhong Y, Shanley J (1995) Altered nerve terminal arborizatoin and synaptic transmission in *Drosophila* mutants of cell adhesion molecule fasciclin I. Journal of Neuroscience 15(10):6679-6887.